

## Alfvén Wave Excitation Due to Pressure Anisotropy in the GAMMA10 Tandem Mirror

NAKAMURA Motoyuki, ICHIMURA Makoto, TANAKA Satoru, KANAZAWA Seikou,  
MOTEGI Shinji, SAOSAKI Soshun, SAKATA Katsuaki, NAKAGAWA Chikahiro,  
KADOYA Kiyoomi, KAWABATA Toshiki, OHTA Yuriko, HOJO Hitoshi,  
MASE Atsushi, TAMANO Teruo and YATSU Kiyoshi  
*Plasma Research Center, University of Tsukuba, Tsukuba, Ibaraki 305-8577, Japan*

(Received: 8 December 1998 / Accepted: 20 May 1999)

### Abstract

Alfvén ion cyclotron (AIC) modes are driven by a strong temperature anisotropy in the case of the high power ion cyclotron range of frequency (ICRF) heating on the GAMMA10 tandem mirror. Parameters on which the AIC modes are observed in the GAMMA10 are much smaller than the theoretically predicted parameters. The axial structure of the AIC modes is measured by magnetic probes and depends strongly on the axial pressure profile. It is suggested that the axial boundary condition is essential for the excitation of the AIC modes.

### Keywords:

tandem mirror, anisotropy, AIC modes, eigen mode, boundary condition, ion distribution

### 1. Introduction

An ion cyclotron range of frequency (ICRF) wave has been effectively used for plasma heating in the GAMMA10 tandem mirror. In the central cell which is a main plasma confinement region, an ion temperature reaches several keV and the temperature anisotropy  $T_{\perp}/T_{\parallel}$  (defined as the temperature ratio of the perpendicular to the parallel to the magnetic field line) becomes above 10. As a result, Alfvén ion cyclotron (AIC) modes are spontaneously excited due to the strong anisotropy [1]. The AIC modes are one of the micro-instability and are in the branch of shear Alfvén wave. Although there are many theoretical works for the AIC modes, there are few experimental studies in the laboratory plasma. The AIC modes in the GAMMA10 tandem mirror are observed in the parameter region above  $\beta_{\perp}(T_{\perp}/T_{\parallel})^2 \sim 0.3$  [2], which is much smaller than the condition for the absolute instability of  $\beta_{\perp}(T_{\perp}/T_{\parallel})^2 \sim 3.52$ , predicted by the present theory [3]. The AIC modes have several discrete

peaks in the frequency spectrum which indicate the excitation of eigen modes in the axial direction. The scattering of ions to the parallel direction due to the AIC modes is predicted theoretically. In the mirror configuration, an increase of the scattering implies the degradation of the confinement. In this paper, we study the excitation mechanism of the AIC modes from the axial structures of the AIC modes and the plasma parameters.

### 2. Experimental Setup

GAMMA10 is the axisymmetrized tandem mirror which consists of five mirror cells. The central cell is the main plasma confinement region where the vacuum chamber has an inner diameter of 1.0 m and a length of 6.0 m and the magnetic field strength in the midplane is 0.41 T. The ICRF antennas for plasma heating are arranged near both ends of central cell and excite the

Corresponding author's e-mail: nakamura@prc.tsukuba.ac.jp

slow wave. The ion cyclotron resonance layers exist near the midplane of the central cell. The slow wave propagates to the resonance layer and transfers the energy to ions via the cyclotron dumping. Two anchor cells for the macroscopic stability are located on both sides of the central cell and two plug/barrier cells for the formation of the confinement potential are located at the outermost region.

Three diamagnetic loops are arranged on the positions of  $z = -0.3$  m,  $z = +1.5$  m and  $z = +1.95$  m to evaluate the axial pressure distribution. The pressure anisotropy is estimated from the diamagnetic loop array by using the axial pressure profile models [4], and MHD equilibrium equation [5]. We measure the magnetic fluctuations generated in the plasmas by using the magnetic probes. The magnetic probes are installed along the magnetic field line and their positions are  $z = -1.12$  m and  $z = -1.28$  m to measure axial structure of the AIC modes. The probe signals are analyzed by using a conventional fast Fourier transform (FFT) method and the axial wave numbers  $k_{\parallel}$  are calculated from the phase difference of two probes.

### 3. Experimental Results and Discussion

#### 3.1 Characteristic of the AIC modes

Figure 1 shows the power spectrum of the magnetic probe signal. The peak of 6.36 MHz in this figure is a wave excited by the ICRF antennas for the plasma heating. The AIC modes are shown below the ion cyclotron frequency, where  $\omega/\Omega_{ci} = 0.8 \sim 0.9$ . The AIC

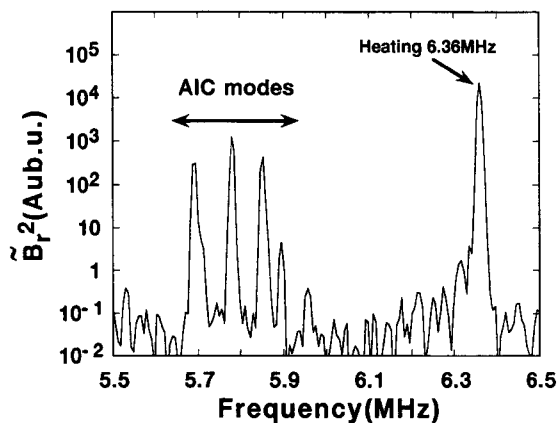


Fig. 1 Power spectrum of the magnetic fluctuations measured by the magnetic probe. The peak of 6.36 MHz is applied ICRF for the plasma heating. AIC modes are excited in the range of  $\omega/\Omega_{ci} = 0.8 \sim 0.9$ .

modes in the GAMMA10 is observed as the eigen modes with discrete peaks in the frequency spectrum. Each peak has different  $k_{\parallel}$  in the initial phase. An existence of the axial boundary condition is suggested. It becomes clear experimentally that the amplitude of the AIC modes depends on  $\beta_{\perp}$  and the temperature anisotropy of ions and is insensitive to the energy distribution of the electrons [6]. This result is consistent with the numerical calculation including the effect of the electron temperature. Figure 2 shows the time evolution of (a) plasma parameters, (b)  $k_{\parallel}$  of each peak of the modes and (c) the amplitude of the AIC modes on the typical discharge. In Fig. 2(a), the value of the diamagnetic signal near the midplane is twice as large as that off-midplane. It means that the central plasma has strong temperature anisotropy. In Fig. 2(b),  $k_{\parallel}$  of each peak approaches to nearly zero from a finite value as increase of the diamagnetic signals. In Fig. 2(c), the amplitude of AIC modes becomes remarkably large when  $k_{\parallel}$  reaches zero. Since the probes are located off-

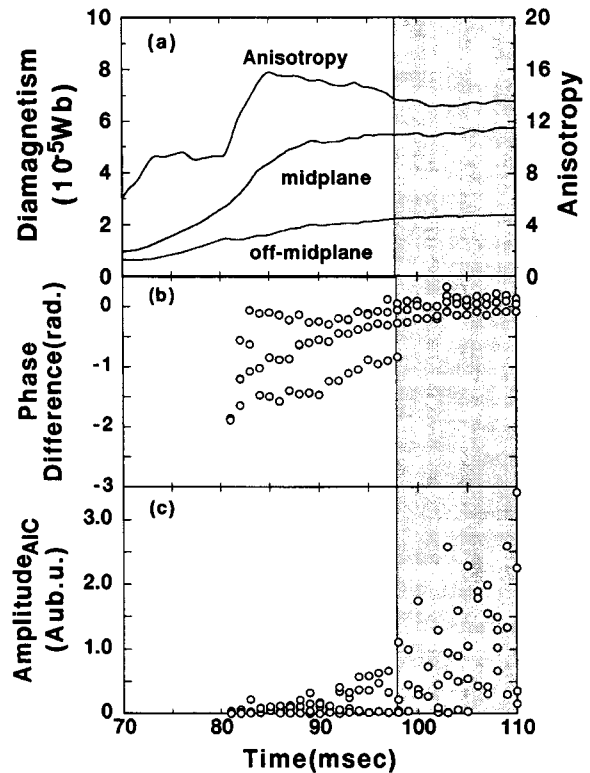


Fig. 2 Time evolution of the plasma parameter on the typical discharge: (a) an anisotropy and the plasma pressure at the midplane and off-midplane in the central cell, (b)  $k_{\parallel}$  of the AIC modes, (c) the amplitude of the AIC modes.

midplane at  $z = -1.12$  m and  $z = -1.28$  m, the variation of  $k_{\parallel}$  indicates that there are two different regions of a propagating wave and a standing wave. The AIC modes are propagating from the midplane in the case of the finite  $k_{\parallel}$ , and become standing waves when  $k_{\parallel} \sim 0$  [7]. In the previous experiment, the AIC modes are observed as the standing wave by inner probes located near  $z = -0.4$  m. It is considered that the boundary of two regions passes through the probe location as increase of the plasma parameters. To clarify the excitation mechanism of the AIC modes, it is necessary to understand parameters of the boundary condition and the reflection mechanism.

### 3.2 Axial boundary conditions of the AIC modes

To find the parameters of the boundary condition, we have analyzed data on the following two experiments. One is an experiment with the different magnetic field strength. In the case, the axial distribution of the plasma pressure changes due to the different location of the cyclotron resonance layer. We employ two magnetic field conditions of 0.41 T and 0.39 T. The location of ICRF resonance layer in the case of 0.39 T exists at the location outer than in the case of 0.41 T. As a result, the axial pressure distribution of 0.39 T is relatively flat in the axial direction. For analysis of the AIC modes, we adopt the experimental conditions with the same diamagnetic signal at the midplane. Figure 3 shows the typical discharges of the two condition. Figure 3(a) shows the temporal evolution of the diamagnetic signals in the central cell on the typical discharges. A solid line indicates the case of 0.41 T and the dotted line 0.39 T. In both cases, the diamagnetic signal at the midplane reaches  $6.0 \times 10^{-5}$  Wb, it means the same pressure at the central cell midplane. Figure 3(b) shows the parameter region of the AIC modes in  $\beta_{\perp}$ -anisotropy space. In this figure, open circles and closed circles mean the cases of 0.41 T and 0.39 T, respectively. The  $\beta_{\perp}$  at the midplane is almost equal and the anisotropy is different in consequence of the location of ICRF resonance layer. Figure 3(c) shows the phase difference between two probes set at  $z = -1.12$  m and  $z = -1.28$  m as a function of the local diamagnetism estimated from the axial pressure distribution. Although the parameter region is different,  $k_{\parallel}$  in both cases closes to 0 at the same value about  $4.5 \times 10^{-5}$  Wb. This suggests that the boundary is determined by the pressure.

Another is an experiment with the different density.

When the electron cyclotron resonance heating (ECRH) in both plug/barrier cells is used for the potential formation, the density in the central cell increases due to the improvement of the confinement. A typical discharge is shown in Fig. 4. Figure 4(a) shows the temporal evolution of the line density, the diamagnetic signal and the anisotropy. An initial plasma is produced and heated by ICRF waves and the potential confinement by ECRH is performed from 130 ms to 190 ms. The density increases during ECRH pulse. Figure 4(b) and 4(c) shows the temporal evolution of the phase difference and the amplitude of the AIC modes, respectively. As mentioned previously, the pressure at the probe location increases when the anisotropy becomes weak in the case of the same diamagnetic signal at the central cell midplane. The boundary

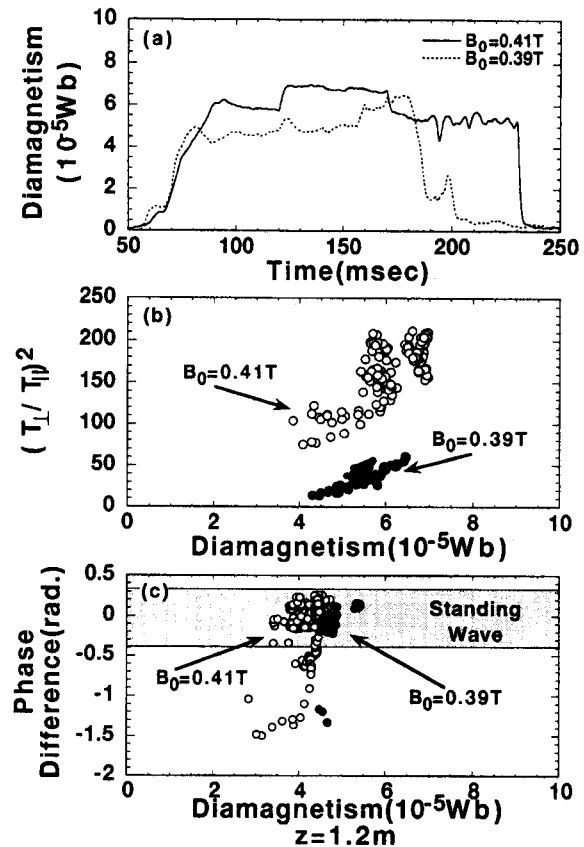


Fig. 3 Plasma parameters in the experiments with the different locations of the ICRF resonance layer: (a) typical diamagnetic signals in both cases: solid line for 0.41 T and dotted line for 0.39 T, (b) parameter region of the AIC modes excitation, (c) the phase difference between two probes as a function of the diamagnetic signals at  $z = -1.2$  m.

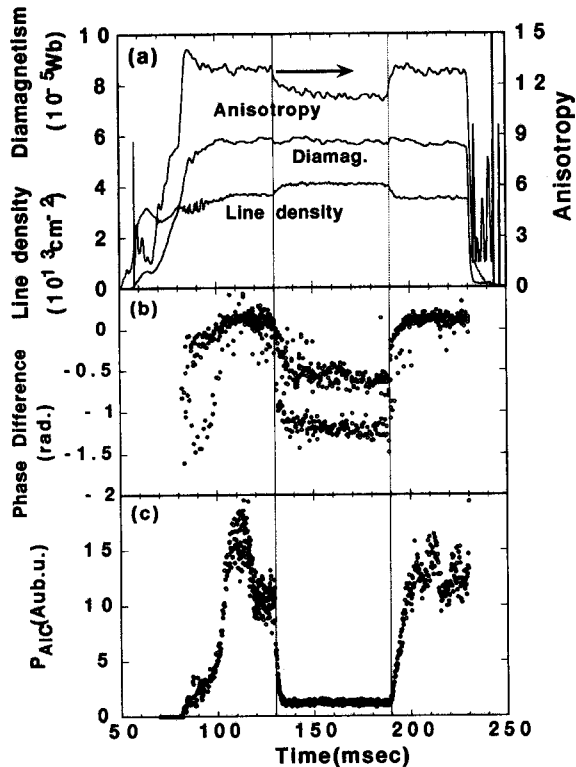


Fig. 4 Plasma parameters in the experiment with the potential confinement. ECRH is applied between 130 ms and 190 ms: (a) the line density, the diamagnetic signal and the anisotropy in the central cell, (b) the phase difference between two probes and (c) the amplitude of the AIC modes.

between the standing wave and the propagating wave regions is expected to still exist outside the probe location. However, Fig. 4(b) shows the phase difference of each mode becomes finite when ECRH is applied. The finite  $k_{\parallel}$  indicates the waves are propagating at the probe location and the boundary moves toward the midplane. When the density increases due to the potential confinement under the condition of the fixed heating power, it is considered the temperature decreases relatively. The increase of the pressure at the probe location is mainly due to the increase of the

density rather than the temperature. The experimental results shown in Fig. 4 indicate the temperature at the probe location decreases and is essential for the mechanism of the wave reflection.

#### 4. Conclusion

The AIC modes are strongly excited in the parameter region above  $\beta_{\perp}(T_{\perp}/T_{\parallel})^2 \sim 0.3$  in the GAMMA10 tandem mirror, which is much smaller than the parameters predicted by the theory. We discussed the excitation of the AIC modes including the axial boundary conditions. The AIC modes have two different regions of the propagating wave and the standing wave. These two regions are definitive element of AIC modes excitation. It is suggested experimentally that the boundary is determined by the axial temperature distribution and is essential for the excitation of the AIC modes in the GAMMA10.

#### Acknowledgements

The authors deeply acknowledge the GAMMA10 group of the University of Tsukuba for their collaboration and stimulating discussions.

#### References

- [1] M. Ichimura *et al.*, Phys. Rev. Lett. **70**, 2734 (1993).
- [2] R. Katsumata, M. Ichimura, M. Inutake, H. Hojo, A. Mase and T. Tamano, Phys. Plasmas **3**, 4489 (1996).
- [3] G.R. Smith, Phys. Fluids **27**, 1499 (1984).
- [4] R. Katsumata, M. Inutake, M. Ichimura, N. Hino, H. Onda, I. Katanuma, H. Hojo, A. Mase and S. Miyoshi, Jpn. J. Appl. Phys. Part.1 **31**, 2249 (1992).
- [5] J.B. Taylor, Phys. Fluids **6**, 1529 (1963).
- [6] M. Nakamura, *et al.*, Jpn. J. Appl. Phys. Part.1 **37**, 342 (1998).
- [7] A. Kumagai, *et al.*, Jpn. J. Appl. Phys. Part.1 **36**, 6978 (1996).